Cell. Mol. Life Sci. (2017) 74:2067–2079
DOI 10.1007/s00018-016-2450-4

Cellular and Molecular Life Sciences

ORIGINAL ARTICLE

WIP1 phosphatase is a critical regulator of adipogenesis through dephosphorylating PPARγ serine 112

Dahu Li[1] · Lijun Zhang[1] · Lun Xu[1] · Lili Liu[1,5] · Yunling He[1] · Yiyao Zhang[1,6] · Xin Huang[1] · Tong Zhao[1] · Liying Wu[1] · Yongqi Zhao[1] · Kuiwu Wu[1] · Hui Li[4] · Xiao Yu[4] · Taiyun Zhao[7] · Shenghui Gong[1] · Ming Fan[1,2,3] · Lingling Zhu[1,2]

Received: 3 August 2016 / Revised: 7 December 2016 / Accepted: 29 December 2016 / Published online: 8 February 2017

Abstract WIP1, as a critical phosphatase, plays many important roles in various physiological and pathological processes through dephosphorylating different substrate proteins. However, the functions of WIP1 in adipogenesis and fat accumulation are not clear. Here, we report that WIP1-deficient mice show impaired body weight growth, dramatically decreased fat mass, and significantly reduced triglyceride and leptin levels in circulation. This dysregulation of adipose development caused by the deletion of WIP1 occurs as early as adipogenesis. In contrast, lentivirus-mediated WIP1 phosphatase overexpression significantly increases the adipogenesis of pre-adipocytes via an enzymatic activity-dependent mechanism. PPARγ is a master gene of adipogenesis, and the phosphorylation of PPARγ at serine 112 strongly inhibits adipogenesis; however, very little is known about the negative regulation of this phosphorylation. Here, we show that WIP1 phosphatase plays a pro-adipogenic role by interacting directly with PPARγ and dephosphorylating p-PPARγ S112 in vitro and in vivo.

Keywords Adipogenesis · Adiposity · Dephosphorylation · PPARγ · WIP1 phosphatase

Abbreviations

aP2	Adipocyte protein 2
C/EBP	CCAAT/enhancer-binding protein
MRI	Magnetic resonance imaging
PPAR	Peroxisome proliferator-activated receptor
WIP1	Wildtpye p53-induced phosphatase 1

Introduction

Obesity has become a threatening epidemic worldwide. Excessive body adiposity often leads to metabolic syndrome, which is a leading cause of death worldwide and is characterized by a series of symptoms, such as dyslipidemia, type 2 diabetes, and cardiovascular disease [1, 2]. Adipose tissue is at the center of metabolic syndrome through its secretion of various adipokines that regulate the circulating lipid levels, insulin sensitivity, appetite and other metabolism processes, while the dysfunctions of adipogenesis, abnormal adipose tissue development and homeostasis correlate closely with metabolism disorders [3]. Adipose development originates from adipogenesis, which is controlled by an elaborate cellular signaling network [4]. Exploring the key molecular signal that link adipogenesis to adipose development is of significant scientific and

Electronic supplementary material The online version of this article (doi:10.1007/s00018-016-2450-4) contains supplementary material, which is available to authorized users.

✉ Ming Fan
fanming@nic.bmi.ac.cn

✉ Lingling Zhu
linglingzhu@hotmail.com

1 Department of Cognitive Science, Institute of Basic Medical Sciences, Beijing 100850, China

2 Co-innovation Center of Neuroregeneration, Nantong University, Nantong 226001, China

3 Beijing Institute for Brain Disorders, Beijing 100069, China

4 Department of Physiology, School of Medicine, Shandong University, Jinan 250012, China

5 Navy General Hospital of PLA, Beijing 100048, China

6 Air Force General Hospital of PLA, Beijing 100142, China

7 Beijing Institute of Pharmacology and Toxicology, Beijing 100850, China

medical importance in understanding the array of metabolism pathologies.

Transcription factor peroxisome proliferator-activated receptor gamma (PPARγ) is a nuclear hormone receptor that is considered a master regulator of adipogenesis, adipose development, and metabolism [4–6]. Previous studies indicated that PPARγ is sufficient to launch adipogenesis [7] and is essential for adipogenesis since PPARγ knockout mouse showed seriously impaired adipose development [8]. Target genes of PPARγ, such as aP2 (adipocyte protein 2) and adipsin, are highly expressed in adipose tissue and account for specialized adipocyte formation and adipose homeostasis. PPARγ activity is under precise and tight regulation, in which posttranscriptional modifications of the PPARγ protein play an indispensable role, including its phosphorylation, ubiquitylation, O-GlcNAcylation, and SUMOylation, with the most well described of these modifications being phosphorylation [9]. In recent years, increasing evidence has revealed that phosphorylation modifications at different sites on the PPARγ protein are vital for the regulation of its activity and can influence its physiological functions, which include adipogenesis, lipid metabolism, and insulin sensitivity [10–13]. However, the only known site-specific phosphorylation that can alter the adipogenic activity of PPARγ is at serine 112, which has been shown to inhibit adipogenesis strongly [12]. Further, except for protein phosphatase 5 [14–16], very little is known about the physiological and cellular intrinsic negative regulators of this phosphorylation.

WIP1 (wildtpye p53-induced phosphatase 1), also called PPM1D, is a serine/threonine phosphatase that belongs to the type 2 C phosphatases family [17]. WIP1 is induced by transcription factor p53 and NF-κB at the transcriptional level, and it is stabilized by BRCA1 signaling and destabilized by miR-16 in response to different types of DNA damage [18]. Compared to the regulatory mechanism of WIP1 itself, the understandings on the function of WIP1 are deeper and wider. In both humans and genetic engineering mouse models, WIP1 has been shown to play many critical roles in tissue development and homeostasis, DNA damage and repair, tumorigenesis, inflammation response, and senescence, in which WIP1 has been proven to alter cellular signal transduction through dephosphorylating several key regulators, such as p53, p38, ATM, NF-κB, and so on [19–25]. A recent study noted that WIP1 deficiency results in resistance to high-fat diet-induced atherosclerosis and obesity, focusing primarily on the roles that WIP1 plays in converting macrophages into foam cells and aorta plaque formation, but it considered little adipose biology [26]. Because high-fat diet feeding is an external stimulus, an adiposity analysis on subjects fed a chow diet provides a better reflection of adipose tissue development and homeostasis under normal circumstances. However, whether WIP1 is involved in adipose tissue development and the generation of adipocytes on a chow diet remains unknown.

In this study, we found that even on a chow diet, WIP1-deficient mice showed impaired body weight growth, dramatically decreased fat mass, and significantly reduced circulating triglyceride and leptin levels. Subsequently, in the analysis of adipogenesis, mouse embryonic fibroblasts (MEFs) from WIP1-deficient mice displayed seriously decreased adipogenic capacities and reductions in critical adipogenic molecular markers expressions, indicating that the impaired adipose development caused by WIP1 depletion occurs as early as adipogenesis. In contrast, lentivirus-mediated WIP1 phosphatase overexpression significantly increased the adipogenesis of pre-adipocyte via an enzymatic activity-dependent mechanism. We further verified that WIP1 plays this pro-adipogenic role by directly interacting with the PPARγ protein and dephosphorylating p-PPARγ S112 in vitro and in vivo, whereas the PPARγ S112A mutation blocked the pro-adipogenic effect of WIP1. Collectively, we identify WIP1 as a novel critical regulator of adipogenesis and fat accumulation, and its pro-adipogenic effect is highly dependent on PPARγ S112.

Materials and methods

Mice maintenance and body weight growth curve measurement

WIP1 knockout (KO) (129Sv-C57BL/6 background) mouse strain was from Dr. Zhi-Cheng Xiao and was originally created by Dr. L.A. Donehower, as described previously [27, 28]. In this study, we backcrossed WIP1 KO mice onto a C57BL/6 background. Mice were maintained under a 14 h light/10 h dark cycle at a constant temperature of 22 °C and fed a chow diet containing 5% fat (Institute of Jingfeng Medical Laboratory Animal) and had free access to food and water except under special conditions, where indicated. From 5 to 25 weeks of age, the bodyweight of WT and KO male mice was measured every 2 weeks. All animal experimental procedures fully complied with the related laboratory animal regulations.

Nuclear magnetic resonance (MRI) analysis

For the precise quantitation of body fat mass and lean mass, mice were measured by Echo MRI Combo-700 Body Composition Analyzer (Echo Medical Systems). The body composition images of mice were acquired using a 7 T MR scanner (Agilent). Briefly, mice were imaged under 1% isoflurane anesthesia using a T1-weighted pulse sequence that rendered fat bright and nonfat tissues dark to facilitate segmentation.

Cell isolation and culture

For MEFs studies, WIP1 heterozygous mice were bred to generate embryonic 13.5–14.5 days littermate WT and KO embryos that were used to derive fibroblasts. In brief, primary MEFs were isolated by removing the heads of the embryos, scratching out the viscera with forceps, and trypsinizing the bodies for 30 min after mincing. The resulting slurry was seeded in culture dishes, and non-adhesive cells were discarded within 3 h. The remaining cells were deemed to be MEFs and were cultured to the 3rd passage for experiments. MEFs and the human embryonic kidney HEK 293T cell line were cultured in DMEM medium containing 10% fetal bovine serum (FBS) (Gibco). The pre-adipocyte cell line 3T3-L1 and fibroblast cell line NIH 3T3 were cultured in DMEM medium containing 10% newborn calf serum (NCS) (Gibco).

Cell transfection, RNAi, plasmid point mutation, lentivirus infection, and stable cell line screening

For exogenous co-immunoprecipitation (Co-IP) and dephosphorylation assays, mouse WIP1 and PPARγ2 expression plasmids were transfected into HEK 293T cells with TurboFect Reagent (Thermo) for 48 h, and the cell samples were harvested for further analysis. WIP1 siRNA and matched transfection regent (Ribo Bio) was applied according to manufacturer's instruction. For lentivirus-mediated overexpression, Flag-tag mouse WIP1 and phosphatase-dead WIP1 point mutants (A95D, D307A) were cloned into pCDH-copGFP-MSCV (CD523A-1) lentiviral vectors (System Biosciences), and Flag-tag mouse PPARγ2 and PPARγ2 S112A were cloned into pCDH-puro-resistant MSCV (CD522A-1) lentiviral vectors (System Biosciences). The corresponding lentivirus outputs of these expression plasmids were infected into 3T3-L1 cell with polybrene (Sigma) assistance to obtain favorable effects. The plasmids of WIP1 point mutants (A95D, D307A) and PPARγ2 S112A were generated with a Muta-direct™ kit (SBS Genetech) according to the manufacture's instruction. For screening stable cell line of expressing PPARγ2 or PPARγ2 S112A, the NIH 3T3 cell was infected with the corresponding lentivirus outputs for 72 h, and then the selective medium containing puromycin (Sigma) with final concentration 5 μg/ml was added and replaced every 2 days. This procedure was continued for 20 days to obtain ideal effects.

Adipogenic differentiation assays

After counting, the same numbers of cells from different cohorts was suspended in adipogenesis induction medium and complete medium and reseeded at the same density to make the cells confluent when they adhered to cell culture clusters. The adipogenesis induction medium consisted of DMEM supplemented with 10% bovine serum (FBS for MEFs, and NCS for 3T3-L1 cells), 10^{-6} M dexamethasone (Sigma), 500 μM 3-isobutyl-1-methylxanthine(Sigma) and 10 μg/ml insulin (Sigma). The complete medium was DMEM medium containing 10% bovine serum (FBS for MEFs, and NCS for 3T3-L1 cells) as described above. To induce adipogenic differentiation, after 2 days of exposure to the induction medium, the cells were cultured in DMEM containing 10% bovine serum and 10 μg/ml insulin, and this medium was renewed every 2 days until the assays were performed. As for spontaneous adipogenic differentiation, the complete medium was also renewed every 2 days. The adipogenic differentiation assay of stable NIH 3T3 cell line was conducted as previously described [7, 12]. Oil red-O staining was performed as described [29]. To quantify adipocytes, we performed adipogenesis assays in 24-well cell culture clusters. After adipogenic induction, oil red-O staining of positive cells of every cohort was counted in 3–5 random visual fields of three replicate wells per cohort.

Real-time quantitative PCR (Q-PCR) analysis

Total RNA was extracted using the Trizol reagent (Sigma). The subsequent reverse transcription reactions were performed using a ReverTra Ace Kit (TOYOBO). Real-time quantitative PCR was performed using an SYBR PCR Master Mix Kit (CW Biotech) and 0.2 μM specific primers in a volume of 15 μl. The data were acquired using an ABI step one plus system (Life Technology). The primer sequences are shown in the Supplemental Materials.

Luciferase reporter assay

The PPARγ luciferase reporter plasmid based on PPRE sequence (Yeasen Biotech) and pRL-TK vector (Promega) that was as an external control were transfected into WIP1 WT and KO MEFs with lipotamine 3000 (Life Technology). After 72 h of transfection, the cells were lysed with passive lysis buffer (Promega), and luciferase activity of sample was measured with a dual luciferase assay system (Promega) in accordance with the manufacturer's protocol. The final data for each sample were calculated by normalizing the PPARγ reporter's luciferase value to pRL-TK vector's luciferase value.

Western blot and immunoprecipitation

MEFs, 3T3-L1 cells, HEK 293T, NIH 3T3 cells, and tissue samples were harvested and lysed in ice-cold TNE buffer (50 mM Tris HCl, pH 7.5; 150 mM NaCl;

1 mM EDTA; and 1% NP-40) containing phosphatase and protease inhibitor cocktails (Roche). Western blot assays were performed using a routine protocol. C/EBPα (D-5), PPARγ (E8), aP2 [A-FABP (B-4)], adipsin (D-8), β-actin (I-19), p-PPARγ S112 (SC-28001) and Flag-HRP [OCTA-probe (D-8)] antibodies were products of Santa Cruz. The antibodies for WIP1 (D4F7), and Myc/Myc-HRP were from Cell Signaling Technology and MBL, respectively. GST and His antibodies were products of CW Biotech. In the analysis of endogenous and exogenous proteins, interactions between WIP1 and PPARγ, 1–2 μg of specific or tag antibody was added to the cell lysate samples and incubated at 4 °C with rotation for 12–24 h. Then, protein A/G-agarose (Santa Cruz) was added, and the samples were rotated for another 12 h to complete the immunoprecipitation. The immunoprecipitate was washed with TNE buffer 3 times (10 min for each washing). Subsequently, both total cell lysates and immunoprecipitates samples were detected by western blot with WIP1 and PPARγ antibodies, or corresponding tag antibodies.

In vitro GST pull-down assay

His-WIP1 and a serial of GST tag mouse proteins (GST, GST-C/EBPα, GST-C/EBPβ and GST-PPARγ2) were expressed in *Escherichia coli* BL21 (DE3). These GST tag proteins were immobilized on glutathione-Sepharose 4B beads (CW Biotech) and washed to remove non-specific binding proteins. The beads were then incubated with Ni-nitrilotriacetate-agarose (GE Lifesciences) purified His-WIP1 protein for 24 h at 4 °C. Subsequently, the beads were washed with GST-binding buffer (100 mM NaCl, 50 mM NaF, 2 mM EDTA, 1% NP40 and protease inhibitor cocktail) to remove non-specific binding. Target protein complexes were eluted with reduced glutathione buffer, and these protein samples were analyzed by western blot.

In vitro protein phosphatase assays

The synthetic phosphopeptide of mouse p-PPARγ2 S112 was customized in SBS Genetech Corporation. The

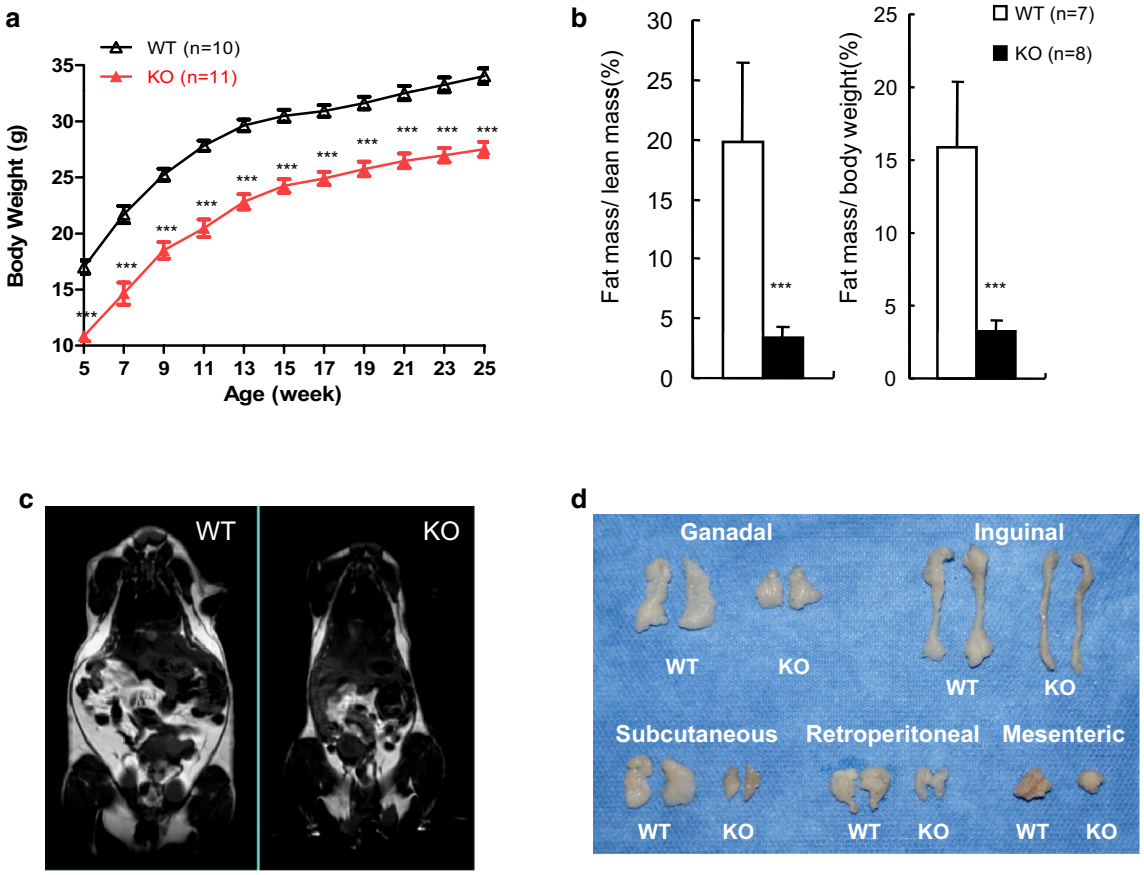

Fig. 1 WIP1-deficient mice show significantly decreased body weight and adiposity. **a** Body weight growth curves of WIP1 WT and KO male mice on a chow diet. The data are shown as the mean ± SEM. **b** MRI measurements of body fat composition and **c** a typical MRI analysis images of WIP1 WT and KO mice at 24 weeks of age. **d** Representative comparative images of the main white adipose pads from WIP1 WT and KO mice at 20 weeks of age. ***$P < 0.001$

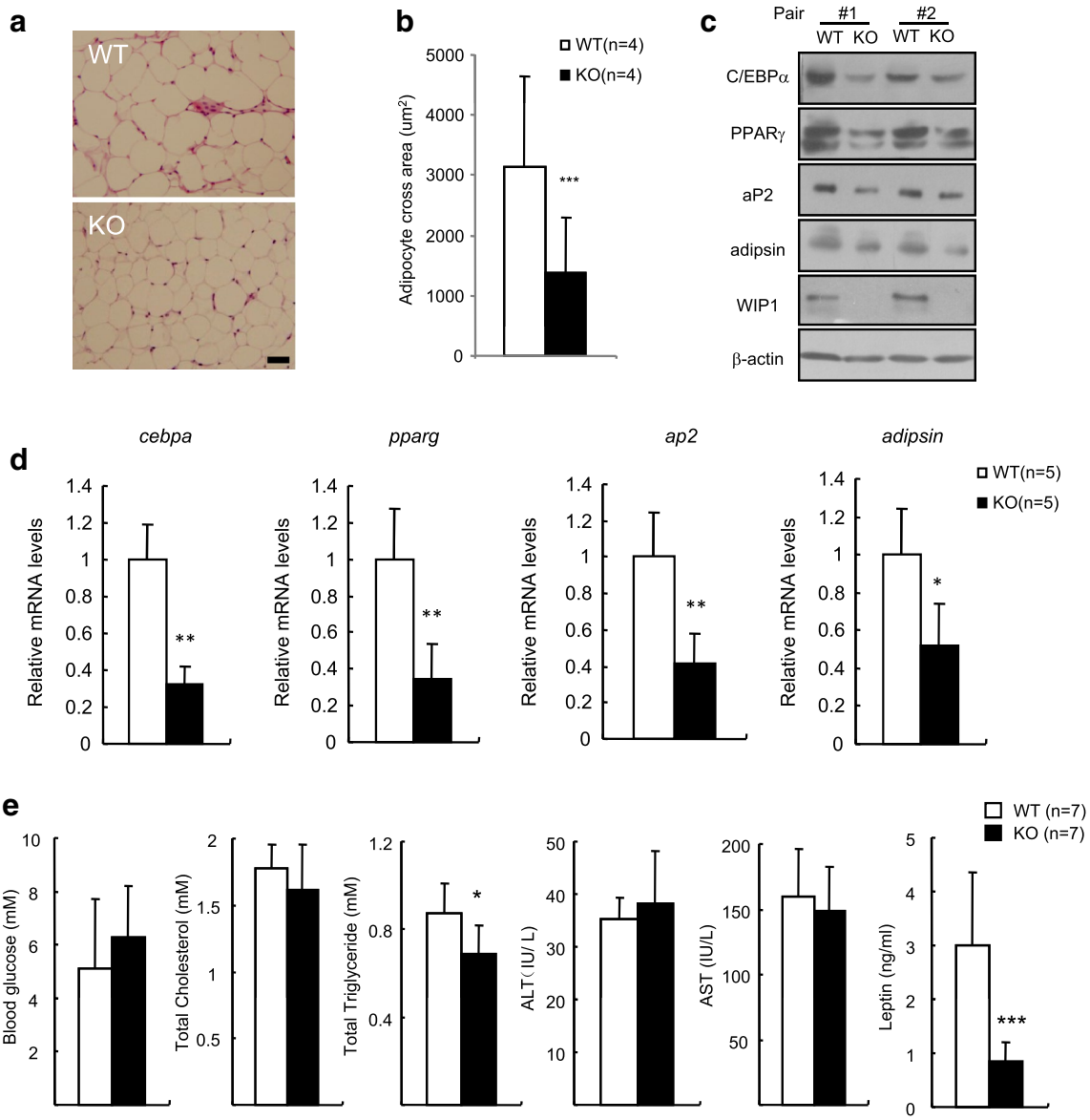

Fig. 2 WIP1-deficient mice exhibit reduced adipocyte size, decreased marker genes expression in adipose tissue and reduced circulating triglyceride and leptin levels. **a** Representative H&E staining and **b** adipocyte size quantitation data of gonadal adipose sections derived from WIP1 WT and KO mice ($n=4$). *Scale bar* 50 μm. **c** Western blot and **d** Q-PCR analyses of several critical maker genes expression in WT and KO gonadal adipose. Q-PCR data were normalized to β-actin mRNA expression ($n=5$). **e** Comparisons of glucose, cholesterol, triglyceride, alanine transaminase (ALT), aspartate aminotransferase (AST) and leptin levels in the serum of WIP1 WT and KO mice ($n = 7$). All quantitative data are presented as the mean ± SD. $^{*}P<0.05$, $^{**}P<0.01$, $^{***}P<0.001$

sequence is listed as follows: KLQEYQSAIKVEPAS̲P-PYYSEKTQLYNRPH (amino acid: 97–127). The underlined S represents the phosphorylated serine 112. According to the method used in the previous report [30], recombinant GST protein, GST-mouse WIP1, and GST-phosphatase dead mouse WIP1 point mutants (A95D, D307A) were purified from bacterial lysates (final amount 0.05 μM), and then diluted in buffer (50 mM Tris–HCl [pH 7.5], 0.1 mM EGTA, and 0.02% 2-mercaptoethanol). Subsequently, each purified recombinant protein was incubated with BSA (1 mg/ml) and 30 mM $MgCl_2$ containing 100 μM phosphopeptide for 20 min at 30 °C. Then, these reaction samples was denatured, and loaded onto 15% gradient SDS–polyacrylamide gel. Proteins were transferred to PVDF membrane (0.2 μm) and detected by GST and p-PPARγ S112 antibodies.

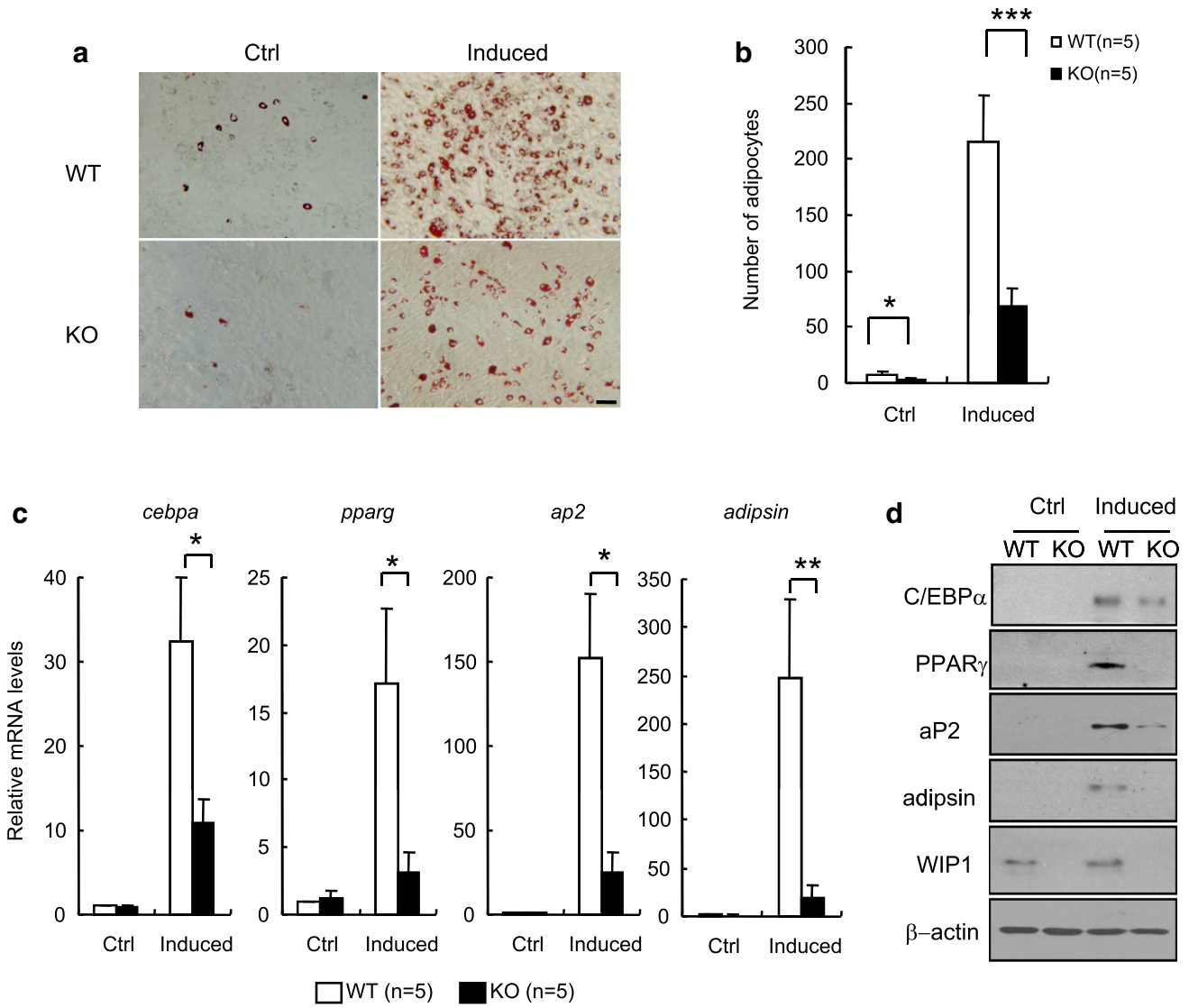
a
Ctrl
Induced
WT
KO
b
***
WT(n=5)
KO(n=5)
Number of adipocytes
300
250
200
150
100
50
0
*
Ctrl
Induced
c
cebpa
pparg
ap2
adipsin
Relative mRNA levels
*
*
*
**
40
30
20
10
0
25
20
15
10
5
0
200
150
100
50
0
350
300
250
200
150
100
50
0
Ctrl
Induced
WT (n=5)
KO (n=5)
d
Ctrl
Induced
WT KO WT KO
C/EBPα
PPARγ
aP2
adipsin
WIP1
β–actin
e
Ctrl
Induced
Negative Control
WIP1 - siRNA
Negative Control (n=3)
WIP1-siRNA (n=3)
Number of adipocytes
100
80
60
40
20
0
*
Ctrl
Induced
Ctrl
Induced
Negative Control + - + -
WIP1 siRNA - + - +
WIP1
β–actin

◂**Fig. 3** WIP1 deficiency or knockdown severely impairs the adipogenic capacity. **a** Oil red-O staining and **b** quantitative data of adipocytes derived from WIP1 WT and KO MEFs after exposure to normal complete medium (Ctrl) or adipogenic induction medium (Induced) for 6–8 days. The images and quantitative data are from a representative experiment of five independent experiments. **c** Q-PCR and **d** western blot analyses of critical adipogenic marker genes expression in the WT and KO MEFs after treatment with complete medium (Ctrl) or adipogenic induction medium (Induced) for 6–8 days. **e** Oil red-O staining and quantitative data of adipocytes after WIP1 knockdown in 3T3-L1 pre-adipocyte cells. The Q-PCR data are from five independent experiments after normalization to β-actin mRNA expression. *Scale bar* 50 μm. All quantitative data are presented as the mean ± SD. $*P<0.05$, $**P<0.01$ and $***P<0.001$

Blood biochemistry tests and leptin analysis

Serum samples from overnight fasted 20-week-old male mice were subjected to laboratory animal biochemical analyzer (Hitachi) to determine the concentrations of blood glucose, total cholesterol, total triglyceride, alanine transaminase (ALT), and aspartate transaminase (AST). The leptin levels in serum were measured using the mouse leptin ELISA kit (R&D) according to manufacturer's instructions.

Histological analysis of adipose tissue and quantitation of adipocytes size

The mouse gonadal adipose tissues were isolated and fixed in 4% paraformaldehyde in PBS and processed for paraffin sections (5 μm) and stained by hematoxylin and eosin (H&E). The images with scale bars collected from H&E stained adipose sections were analyzed using the Image-Pro Plus 6.0 software to measure and calculate the cross-sectional area of the adipocytes.

Statistical analysis

The data were analyzed using Student's *t* test, except where otherwise indicated. The Q-PCR data of adipogenesis comparisons between WT and KO MEFs or the manipulated stable cell lines cohorts were analyzed using a paired Student's *t* test. Growth curves were analyzed using a two-way ANOVA with Bonferroni's post-test. $P<0.05$ was considered statistically significant.

Results

WIP1 loss leads to significant reductions in body weight and adiposity

Although previous work noted that WIP1 deficiency leads to obesity and arteriosclerosis resistance with high-fat diet feeding due to the dysfunction of macrophage autophagy [26], the function of WIP1 in adipose tissue and adipocytes on a high-fat diet was not determined. Moreover, because high-fat diet feeding is an external stimulus, an analysis of adiposity on a chow diet is a better reflection of adipose development and homeostasis under normal circumstances. We traced the body weight changes of WIP1 wildtype (WT) and knockout (KO) mice fed a chow diet. Strikingly, we found that the body weight of WIP1 KO mice was significantly decreased compared to their WT counterparts from 5 weeks of age and that this difference lasted until the end of our observation period, at 25 weeks of age (Fig. 1a). To determine the contribution of the adipose tissue to this significant difference in body weight, we employed magnetic resonance imaging (MRI) to analyze the body composition of WIP1 WT and KO mice. MRI analysis showed that the critical adiposity indexes of WIP1 KO mice (fat mass/lean mass and fat mass/body weight) decreased approximately three- to fourfold compared to WT mice (Fig. 1b). The MRI images also showed a notable reduction of adipose mass in WIP KO mice (Fig. 1c). In addition, we compared the sizes of the five main murine adipose pads of WIP1 WT and KO mice. The results demonstrated that all of these adipose pads showed dramatic decreases in size in the WIP1 KO mice (Fig. 1d).

WIP1-deficient mice show decreased adipocyte size, reduced critical marker genes expression in adipose and reduced circulating triglyceride and leptin

Based on the above observations, we further analyzed adipose tissue sections of WIP1 WT and KO mice after H&E staining. The images showed that WIP1 deficiency led to smaller adipocytes compared to WT mice (Fig. 2a), a difference that was statistically significant according to the Image-Pro Plus software measurement and calculation (Fig. 2b). Because an unusual cell morphology often results from dysregulated molecular events, we compared the expression of several critical marker genes between WT and KO adipose tissues. It is well known that the transcription factors C/EBPα (CCAAT/enhancer-binding protein alpha) and PPARγ are master genes of adipogenesis and are critical for adipose homeostasis [4, 31]. Target genes of PPARγ, such as aP2 and adipsin, are also known to be expressed predominantly in adipose and are important for specialized adipocyte formation and the maintenance of adipose tissue function. Our results revealed that the expression levels for these critical proteins decreased in WIP1 KO samples compared to WT samples (Fig. 2c). Further, through real-time quantitative PCR (Q-PCR) assays, we found that these expression differences between WT and KO adipose samples occurred at the transcription level (Fig. 2d). It is known that metabolic disorders are

often associated with abnormal adipose development. We thus also tested the impacts of WIP1 loss on the circulating levels of glucose, total cholesterol, total triglyceride, alanine transaminase (ALT), and aspartate transaminase (AST). The serum triglyceride levels of KO mice were significantly lower than those of WT mice, whereas the other parameters were comparable between WT and KO mice (Fig. 2e), which suggested that WIP1 was most likely to affect lipid metabolism. In addition, adipose secretes a variety of adipokines to regulate metabolism and other physiological processes. Among these adipokines, the circulating leptin levels were deemed to be a direct reflection of adipose mass, despite their function in regulating metabolism [32]. Our results show that the leptin levels in the serum of KO mice were severely decreased and were almost two times lower than those of their WT counterparts (Fig. 2e). Collectively, these analyses of adipose and blood chemistry were consistent with the above findings that WIP1 deficiency led to significant reduced adiposity and a lean phenotype.

WIP1 deficiency or knockdown results in serious defective adipogenic capacity

It is well known that adipose tissue development correlates closely with early stage adipogenesis and that dysfunctional adipogenic capacity precursor cells lead to adipose tissue abnormalities [4, 31]. Because WIP1 KO mice show serious reductions of adipose mass, body adiposity, and the expression of critical marker genes in adipose, we investigated whether these alterations had any association with early abnormalities in adipogenesis. Primary mouse embryonic fibroblasts (MEFs) and the pre-adipocyte cell line 3T3-L1 are commonly used precursor cell models for adipogenesis research, with the MEFs model reflecting earlier adipogenic capacity [4, 31]. These precursor cells usually display very low spontaneous adipogenic differentiation efficiency in normal complete medium, thus giving rise to very few mature adipocytes, but they show highly efficient adipogenic differentiation upon exposure to induction medium. We isolated WIP1 WT and KO MEFs to compare the alterations in adipogenic capacity caused by WIP1 loss. Our results indicated that, for both spontaneous (Fig. 3a, Ctrl) and induced adipogenic differentiation (Fig. 3a, Induced), WIP1 KO MEFs showed significantly less differentiation to mature adipocytes (oil red-O staining positive cells; Fig. 3b). Further, we used Q-PCR assays to measure the mRNA levels of adipogenic marker genes, such as the adipogenic 'master genes' C/EBPα and PPARγ, and those genes accounting for specialized adipocytes formation, such as aP2 and adipsin. The results revealed that in spontaneous adipogenic differentiation, these genes were expressed at a very low level both in WT and KO MEFs (Fig. 3c, Ctrl). After induction, the expression of these mRNAs was upregulated (Fig. 3c, Induced). However, compared to induced WT MEFs, the mRNA levels of these marker genes in induced KO MEFs were significantly lower: C/EBPα declined approximately threefold, PPARγ declined approximately fourfold, aP2 declined approximately fourfold, and adipsin declined approximately tenfold (Fig. 3c, Induced). Correspondingly, the protein levels of these adipogenic markers in induced KO MEFs also showed expression patterns similar to their mRNA levels (Fig. 3d, Induced). In addition, in the pre-adipocyte cell line 3T3-L1 model, we observed a similar suppression of adipogenesis when WIP1 was knocked down (Fig. 3e).

WIP1 overexpression promotes adipogenesis in a phosphatase activity-dependent way

We further explored whether WIP1 overexpression could alter the adipogenic capacity and whether WIP1 could regulate adipogenesis, depending on its phosphatase activity. The lentivirus-mediated expressions of WIP1, and phosphatase-dead WIP1 point mutants (A95D, D307A) were introduced into the pre-adipocyte cell line 3T3-L1 along with a null vector control, and their effects on adipogenesis were assessed. The spontaneous adipogenic differentiation in normal complete medium was not different in the formation of mature adipocytes (Fig. 4a, b, Ctrl) or in the protein/mRNA expression of adipogenic marker genes (Fig. 4c, d, Ctrl) among the WIP1, mutant WIP1, and null control cohorts. However, after the induction of adipogenesis, the WIP1 overexpression cohort displayed significantly more mature adipocytes (Fig. 4a, b, Induced) and elevated protein and mRNA levels of adipogenic marker genes compared to the null vector cohort (Fig. 4c, d, Induced). It is worth noting that after induction, the mutant WIP1 cohort did not demonstrate enhanced adipogenic capacity, as the WIP1 cohort did, in either adipocyte formation or adipogenic marker genes expression (Fig. 4a–d, Induced). These results strongly suggest that WIP1 promotes adipogenesis via a phosphatase activity-dependent mechanism.

WIP1 interacts with PPARγ directly

Considering the above results, we hypothesized that WIP1 regulates adipogenesis through the dephosphorylation of a critical substrate protein, which plays an important role in adipogenesis. The crucial adipogenic transcription factors, C/EBPα and PPARγ are deemed 'master genes' in adipogenesis [4, 31]. In addition, another member of C/EBPs family, C/EBPβ, is also a relatively important adipogenic transcription factor [4, 31]. Thus, by using GST-pulldown assays, we screened for a possible WIP1 interacting protein among these

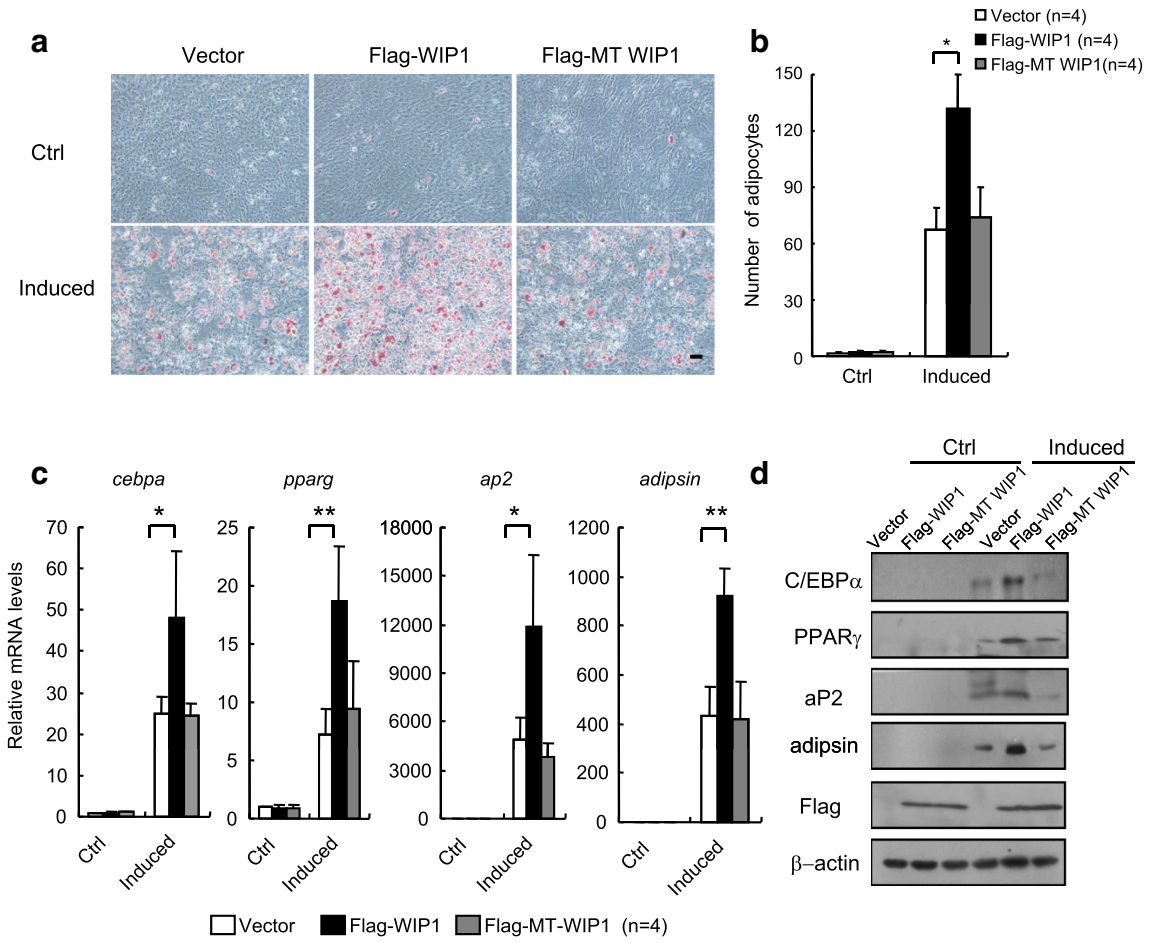

Fig. 4 WIP1 overexpression promotes adipogenesis via a phosphatase activity-dependent mechanism. **a** Oil red-O staining and **b** quantitative data of adipocytes derived from 3T3-L1 pre-adipocyte cells infected with lentiviruses expressing Flag-WIP1 and Flag-WIP1 dead enzyme mutant (Flag-MT WIP1) or null vector control, respectively, treated with complete medium (Ctrl) or adipogenic induction medium (Induced) after 8 days. The images and quantitation data are from a representative result of four independent experiments. *Scale bar* 50 μm. **c** Q-PCR and **d** western blot analyses of critical adipogenic marker genes expression in the Flag-WIP1, Flag-MT WIP1 and vector control cohorts after the same treatments mentioned above. The PCR data are from four representative independent experiments after normalization to β-actin mRNA expression. All quantitative data are presented as the mean ± SD. $*P < 0.05$ and $**P < 0.01$

critical adipogenic transcription factors. Strikingly, we found that recombinant His-WIP1 interacted specifically with GST-PPARγ but not with C/EBPα or C/EBPβ (Fig. 5a). This result suggested that there is a direct interaction between WIP1 and PPARγ recombinant proteins in vitro. Further, we found that the protein interaction between WIP1 and PPARγ could be readily detected when they were ectopically expressed in eukaryotic cells (Fig. 5b). Further, the endogenous protein interaction between WIP1 and PPARγ was observed in adipogenic differentiated MEFs, which indicates that WIP1 can physiologically interact with PPARγ (Fig. 5c).

WIP1 dephosphorylates p-PPARγ S112, and this dephosphorylation is crucial for the pro-adipogenic effect of WIP1

Based on the above observations, we speculated that the PPARγ protein may be a substrate of phosphatase WIP1 in the adipogenesis process and that WIP1 dephosphorylates the PPARγ protein to alter the adipogenic activities of PPARγ. Of the known phosphorylation sites in the PPARγ protein, p-PPARγ S112 is the only one known to be a site that inhibits adipogenesis [9, 12]. We hypothesized that WIP1 dephosphorylates p-PPARγ S112 to promote adipogenic activities of PPARγ. When WIP1 is deficient, the hyper-phosphorylation of PPARγ S112 occurs, which leads to reduced adipogenic activities of PPARγ, subsequent defective adipogenesis, and eventual reduced fat mass.

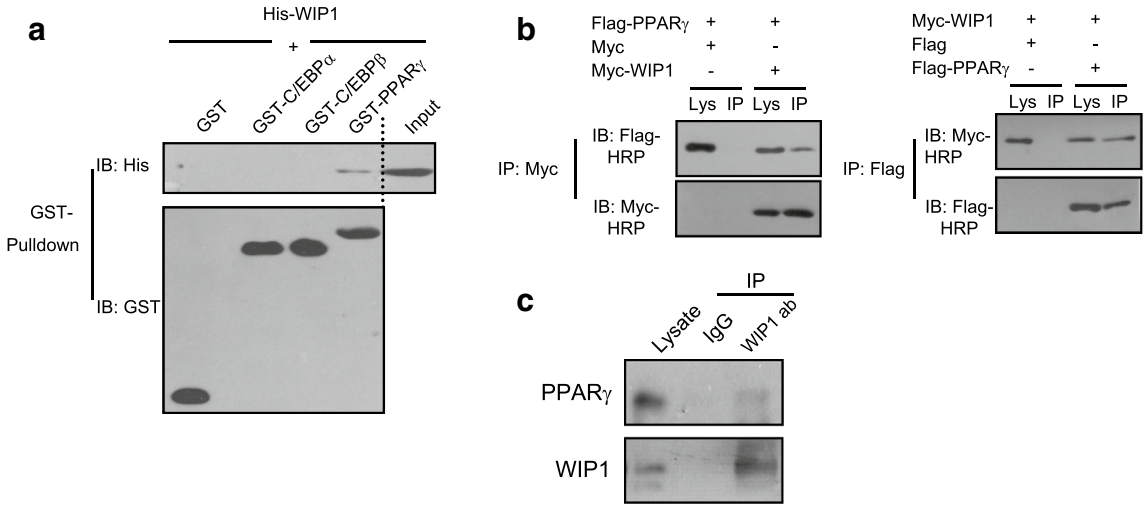

Fig. 5 WIP1 interacts with PPARγ. **a** GST pull-down assays were performed to analyze the interactions between WIP1 and C/EBPα, C/EBPβ, or PPARγ proteins. **b** Exogenous Co-IP assays were employed to detect interactions between ectopically expressed WIP1 and PPARγ proteins in HEK 293T cells. On the *left* is Myc antibody immunoprecipitation, and on the *right* is Flag antibody immunoprecipitation. *Lys* lysate, *IP* immunoprecipitation or immunoprecipitate. **c** Endogenous Co-IP assay analysis of the physiological interaction of WIP1 and PPARγ in adipogenic differentiated MEFs

To verify this hypothesis, we first examined the effect of recombinant WIP1 protein on a synthetic phosphopeptide of PPARγ S112 in vitro. Recombinant wildtype WIP1, but not phosphatase-dead mutant WIP1, can dephosphorylate PPARγ S112 (Fig. 6a). In addition, a markedly decreased level of ectopically expressed p-PPARγ S112 was observed in HEK 293T cells in the presence of WIP1 (Fig. 6b). Similarly, the p-PPARγ S112 level was significantly reduced in 3T3-L1 cells stably expressing WIP1 compared to the control vector and phosphatase-dead mutant WIP1 counterparts after adipogenic induction (Fig. 6c). Moreover, in the knockout mouse model, the level of p-PPARγ S112 in WIP1 KO adipose tissue was higher than that observed in WT (Fig. 6d). Because p-PPARγ S112 seriously inhibits the adipogenic transcriptional activity of PPARγ [12] and WIP1 can dephosphorylate p-PPARγ S112, we further evaluated the impact of WIP1 loss on the transcriptional activity of PPARγ by using a luciferase reporter, with its expression controlled by a PPRE response element, a consensus sequence of PPAR-γ regulated gene. The results revealed that for WIP1 KO MEFs, the transcription activity of PPARγ was significantly decreased in adipogenesis (Fig. 6e). In addition, we investigated whether the pro-adipogenic function of WIP1 relies on p-PPARγ S112. According to previous reports, NIH-3T3 cells have no PPARγ expression or adipogenic capacity, but ectopic PPARγ expression can restore the adipogenic capacity [7, 12]. Thus, this method has been commonly used to verify PPARγ-related regulation. We introduced the lentivirus-mediated plasmid expressing PPARγ and PPARγ S112A mutant into NIH-3T3 cells. Subsequently, WIP1 protein was introduced into these PPARγ- and PPARγ S112A-expressing NIH-3T3 cells, and its impact on adipogenesis was assessed. These experiments showed that WIP1 significantly enhanced adipogenesis in the presence of PPARγ, but has no significant effect when PPARγ S112 can no longer be phosphorylated (S112A) (Fig. 6f).

These findings suggest that PPARγ protein is a physiological substrate of the WIP1 phosphatase and that WIP1-regulated adipogenesis is highly dependent on the dephosphorylation of p-PPARγS112.

Discussion

According to a previous study, WIP1 knockout mice were smaller [27], but their adipose tissue and body composition has not previously been studied. A recent study found that WIP1 deficiency resulted in atherosclerosis and obesity resistance in subjects given a high-fat diet; this study focused primarily on WIP1's roles in the conversion of macrophage to foam cells and aorta plaque formation, but provided little information on adipose biology [26]. Because high-fat diet feeding is an external stimulus, an analysis of adiposity on a chow diet better reflects adipose development and homeostasis under normal circumstances. Our results, which were obtained using a chow diet, revealed that WIP1 deletion result in seriously impairs bodyweight growth and reduces the adipose mass and adiposity indexes. These findings collectively suggested that WIP1 deficiency leads to a lean phenotype, not just a small phenotype, as previously reported. Further, in the commonly

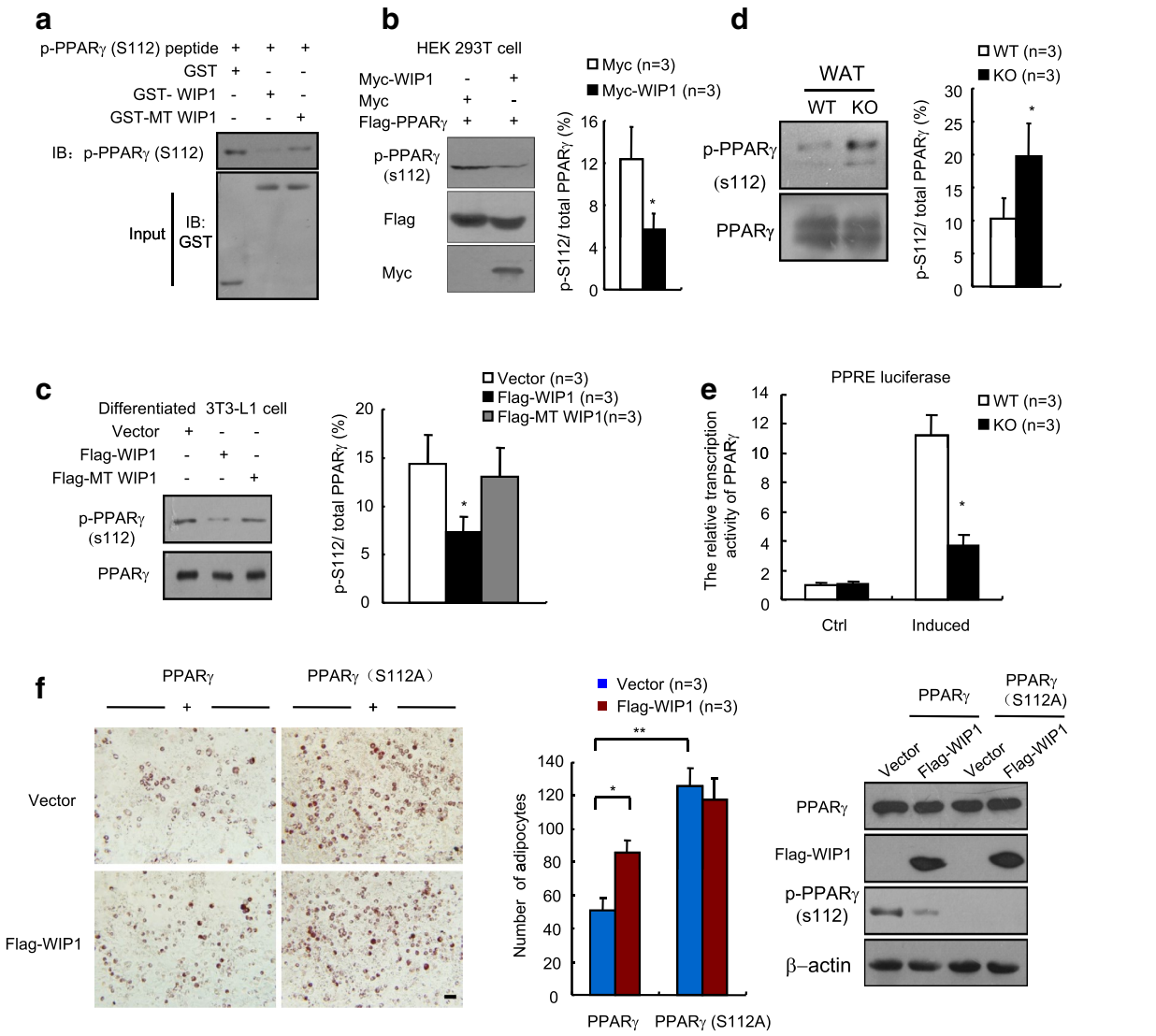

Fig. 6 WIP1 dephosphorylates p-PPARγ S112, and this dephosphorylation is crucial for the pro-adipogenic effect of WIP1. **a** In vitro dephosphorylation assay of GST-WIP1 and GST-WIP1 dead enzyme mutant (GST-MT WIP1) on a synthetic phosphopeptide of PPARγ S112. Western blot analyses of the impact of WIP1 on the phosphorylation of exogenously expressed p-PPARγ S112 in HEK 293T cells (**b**) and adipogenic differentiated 3T3-L1 cells (**c**). **d** The p-PPARγ S112 levels in WIP1 WT and KO adipose tissues. **e** Luciferase reporter assay of transcription activity of PPARγ in WIP1 KO MEFs by measuring PPRE luciferase values. **f** Oil red-O staining, quantitative data of adipocytes, and western blot analysis of the impact of WIP1 on adipogenesis in the presence of PPARγ or PPARγ S112A in NIH 3T3 cells. *Scale bar* 50 μm. All quantitative data are presented as the mean ± SD. $^{*}P < 0.05$ and $^{**}P < 0.01$

used adipogenesis model, primary cultured MEFs, we found that WIP1 null MEFs displayed significant defects in adipogenic differentiation, which suggests that abnormal adipose development in WIP1 KO mice occurred as early as adipogenesis. In addition, according to a previous study, WIP1-deficient MEFs have a decreased proliferation rate and appear to be compromised when entering mitosis [27], with this being the first indication that WIP1 plays a role in cell proliferation. However, the mechanism by which WIP1 functions in cell differentiation is unknown. Our study is the first to prove that WIP1 plays a critical role in adipogenic differentiation and is the first to verify that cell type differentiation is regulated by WIP1.

Concerning WIP1 overexpression leading to increased adipogenesis, we found that WIP1 executed this function via a phosphatase activity-dependent mechanism. In subsequent assays, PPARγ was confirmed to be a protein that interacted with WIP1, and p-PPARγ S112 could be dephosphorylated by WIP1 both in vitro and in vivo. The phosphorylation of PPARγ at serine 112 previously has proven

to strongly suppress adipogenesis, and a serine-to-alanine mutation at this site (S112A) blocked the phosphorylation and significantly promoted adipogenesis in vitro [12]. Mice carrying the PPARγ S112A mutation displayed increased adipogenesis in MEFs and improved insulin sensitivity in the setting of high-fat diet-induced obesity, but exhibited normal adiposity on a chow diet [13]. Our results indicate that the p-PPARγ S112 level in the WIP1 KO mice samples was higher than that in WT samples, indicating that WIP1 deletion results in the hyperactivation of p-PPARγ S112. Because the PPARγ S112A mutation blocked this phosphorylation, we considered that the hyperactive p-PPARγ S112 level accounted for the more seriously reduced adipogenesis and adiposity in WIP1 KO mice on a chow diet. Other researchers have also found that WIP1 KO mice displayed impaired insulin sensitivity when subjected to insulin tolerance tests on a chow diet [33]. Moreover, in the present study, we prove that WIP1 plays the pro-adipogenic role relies on its phosphatase activity and PPARγ S112 in 3T3-L1 and NIH 3T3 cell models. Collectively, our findings of WIP1-associated phenotypes and regulatory mechanisms on adipogenesis and adipose development are consistent with previous studies and provide additional understanding on the mechanisms of action of WIP1. We also observed that WIP1 expression increases during adipogenesis (Supplemental Figure S1). Moreover, in the adipose tissue of obese *ob*/*ob* mouse model, we found upregulated WIP1 expression (Supplemental Figure S2). These results provide interesting clues for future investigations into the medical relevance of WIP1 expression and obesity.

Recently, the phosphorylation of other sites in PPARγ protein, such as serine 273, was shown to specifically regulate insulin sensitivity, but had no effect on adipogenesis [10, 11]. Moreover, some chemical compounds targeting this phosphorylation revealed promising clinical application prospect [10, 11]. Whether WIP1 phosphatase has any effect on these novel phosphorylation sites in PPARγ protein and plays important roles in other aspects of glucose and lipid metabolism or adipose physiology may be interesting questions to explore in the future.

Acknowledgements We greatly appreciate Dr. Zhi-Cheng Xiao for providing WIP1 KO mice strain, Dr. Kai Gao (Institute of Laboratory Animal Science, Chinese Academy of Medical Sciences) for providing technical assistance in MRI assay, and the couple of Dr. Ming Shi and Dr. Dan Liu for providing technical supports in molecular biology.

Compliance with ethical standards

Funding This work was supported by Chinese National Basic Research Development Program (No. 2011CB910802) and National Natural Science Foundation of China (Nos. 31401000 and 81430044).

Conflict of interest The authors declare no conflict of interest.

References

1. Mokdad AH, Ford ES, Bowman BA, Dietz WH, Vinicor F, Bales VS, Marks JS (2003) Prevalence of obesity, diabetes, and obesity-related health risk factors, 2001. Jama 289(1):76–79
2. Bray GA, Bellanger T (2006) Epidemiology, trends, and morbidities of obesity and the metabolic syndrome. Endocr 29(1):109–117. doi:10.1385/ENDO:29:1:109
3. Rosen ED, Spiegelman BM (2014) What we talk about when we talk about fat. Cell 156(1–2):20–44. doi:10.1016/j.cell.2013.12.012
4. Tang QQ, Lane MD (2012) Adipogenesis: from stem cell to adipocyte. Annu Rev Biochem 81:715–736. doi:10.1146/annurev-biochem-052110-115718
5. Willson TM, Lambert MH, Kliewer SA (2001) Peroxisome proliferator-activated receptor gamma and metabolic disease. Annu Rev Biochem 70:341–367. doi:10.1146/annurev.biochem.70.1.341
6. Lefterova MI, Haakonsson AK, Lazar MA, Mandrup S (2014) PPARgamma and the global map of adipogenesis and beyond. Trends Endocrinol Metabol TEM 25 (6):293–302. doi:10.1016/j.tem.2014.04.001
7. Tontonoz P, Hu E, Spiegelman BM (1994) Stimulation of adipogenesis in fibroblasts by PPAR gamma 2, a lipid-activated transcription factor. Cell 79(7):1147–1156
8. Imai T, Takakuwa R, Marchand S, Dentz E, Bornert JM, Messaddeq N, Wendling O, Mark M, Desvergne B, Wahli W, Chambon P, Metzger D (2004) Peroxisome proliferator-activated receptor gamma is required in mature white and brown adipocytes for their survival in the mouse. Proc Natl Acad Sci USA 101(13):4543–4547. doi:10.1073/pnas.0400356101
9. Floyd ZE, Stephens JM (2012) Controlling a master switch of adipocyte development and insulin sensitivity: covalent modifications of PPARgamma. Biochim Biophys Acta 1822(7):1090–1095. doi:10.1016/j.bbadis.2012.03.014
10. Choi JH, Banks AS, Estall JL, Kajimura S, Bostrom P, Laznik D, Ruas JL, Chalmers MJ, Kamenecka TM, Bluher M, Griffin PR, Spiegelman BM (2010) Anti-diabetic drugs inhibit obesity-linked phosphorylation of PPARgamma by Cdk5. Nature 466(7305):451–456. doi:10.1038/nature09291
11. Choi JH, Banks AS, Kamenecka TM, Busby SA, Chalmers MJ, Kumar N, Kuruvilla DS, Shin Y, He Y, Bruning JB, Marciano DP, Cameron MD, Laznik D, Jurczak MJ, Schurer SC, Vidovic D, Shulman GI, Spiegelman BM, Griffin PR (2011) Antidiabetic actions of a non-agonist PPARgamma ligand blocking Cdk5-mediated phosphorylation. Nature 477(7365):477–481. doi:10.1038/nature10383
12. Hu E, Kim JB, Sarraf P, Spiegelman BM (1996) Inhibition of adipogenesis through MAP kinase-mediated phosphorylation of PPARgamma. Science 274(5295):2100–2103
13. Rangwala SM, Rhoades B, Shapiro JS, Rich AS, Kim JK, Shulman GI, Kaestner KH, Lazar MA (2003) Genetic modulation of PPARgamma phosphorylation regulates insulin sensitivity. Dev Cell 5(4):657–663
14. Hinds TD Jr, Stechschulte LA, Cash HA, Whisler D, Banerjee A, Yong W, Khuder SS, Kaw MK, Shou W, Najjar SM, Sanchez ER (2011) Protein phosphatase 5 mediates lipid metabolism through reciprocal control of glucocorticoid receptor and peroxisome proliferator-activated receptor-gamma (PPARgamma). J Biol Chem 286(50):42911–42922. doi:10.1074/jbc.M111.311662
15. Grankvist N, Honkanen RE, Sjoholm A, Ortsater H (2013) Genetic disruption of protein phosphatase 5 in mice prevents high-fat diet feeding-induced weight gain. FEBS Lett 587 (23):3869–3874. doi:10.1016/j.febslet.2013.10.022

16. Jacob W, Rosenzweig D, Vazquez-Martin C, Duce SL, Cohen PT (2015) Decreased adipogenesis and adipose tissue in mice with inactivated protein phosphatase 5. Biochem J 466(1):163–176. doi:10.1042/BJ20140428
17. Zhu YH, Bulavin DV (2012) Wip1-dependent signaling pathways in health and diseases. Prog Mol Biol Transl Sci 106:307–325. doi:10.1016/B978-0-12-396456-4.00001-8
18. Lowe J, Cha H, Lee MO, Mazur SJ, Appella E, Fornace AJ Jr (2012) Regulation of the Wip1 phosphatase and its effects on the stress response. Frontiers in bioscience 17:1480–1498
19. Yi W, Hu X, Chen Z, Liu L, Tian Y, Chen H, Cong YS, Yang F, Zhang L, Rudolph KL, Zhang Z, Zhao Y, Ju Z (2015) Phosphatase Wip1 controls antigen-independent B-cell development in a p53-dependent manner. Blood 126(5):620–628. doi:10.1182/blood-2015-02-624114
20. Zhu Y, Demidov ON, Goh AM, Virshup DM, Lane DP, Bulavin DV (2014) Phosphatase WIP1 regulates adult neurogenesis and WNT signaling during aging. J Clin Invest 124(7):3263–3273. doi:10.1172/JCI73015
21. Ruark E, Snape K, Humburg P, Loveday C, Bajrami I, Brough R, Rodrigues DN, Renwick A, Seal S, Ramsay E, Duarte Sdel V, Rivas MA, Warren-Perry M, Zachariou A, Campion-Flora A, Hanks S, Murray A, Ansari Pour N, Douglas J, Gregory L, Rimmer A, Walker NM, Yang TP, Adlard JW, Barwell J, Berg J, Brady AF, Brewer C, Brice G, Chapman C, Cook J, Davidson R, Donaldson A, Douglas F, Eccles D, Evans DG, Greenhalgh L, Henderson A, Izatt L, Kumar A, Lalloo F, Miedzybrodzka Z, Morrison PJ, Paterson J, Porteous M, Rogers MT, Shanley S, Walker L, Gore M, Houlston R, Brown MA, Caufield MJ, Deloukas P, McCarthy MI, Todd JA, Breast, Ovarian Cancer Susceptibility C, Wellcome Trust Case Control C, Turnbull C, Reis-Filho JS, Ashworth A, Antoniou AC, Lord CJ, Donnelly P, Rahman N (2013) Mosaic PPM1D mutations are associated with predisposition to breast and ovarian cancer. Nature 493(7432):406–410. doi:10.1038/nature11725
22. Filipponi D, Muller J, Emelyanov A, Bulavin DV (2013) Wip1 controls global heterochromatin silencing via ATM/BRCA1-dependent DNA methylation. Cancer cell 24(4):528–541. doi:10.1016/j.ccr.2013.08.022
23. Chew J, Biswas S, Shreeram S, Humaidi M, Wong ET, Dhillion MK, Teo H, Hazra A, Fang CC, Lopez-Collazo E, Bulavin DV, Tergaonkar V (2009) WIP1 phosphatase is a negative regulator of NF-kappaB signalling. Nat Cell Biol 11(5):659–666. doi:10.1038/ncb1873
24. Lu X, Ma O, Nguyen TA, Jones SN, Oren M, Donehower LA (2007) The Wip1 Phosphatase acts as a gatekeeper in the p53-Mdm2 autoregulatory loop. Cancer cell 12(4):342–354. doi:10.1016/j.ccr.2007.08.033
25. Zhang L, Liu L, He Z, Li G, Liu J, Song Z, Jin H, Rudolph KL, Yang H, Mao Y, Zhang L, Zhang H, Xiao Z, Ju Z (2015) Inhibition of wild-type p53-induced phosphatase 1 promotes liver regeneration in mice by direct activation of mammalian target of rapamycin. Hepatology 61(6):2030–2041. doi:10.1002/hep.27755
26. Le Guezennec X, Brichkina A, Huang YF, Kostromina E, Han W, Bulavin DV (2012) Wip1-dependent regulation of autophagy, obesity, and atherosclerosis. Cell Metab 16(1):68–80. doi:10.1016/j.cmet.2012.06.003
27. Choi J, Nannenga B, Demidov ON, BulavIN DV, Cooney A, Brayton C, Zhang Y, Mbawuike IN, Bradley A, Appella E, Donehower LA (2002) Mice deficient for the wild-type p53-induced phosphatase gene (Wip1) exhibit defects in reproductive organs, immune function, and cell cycle control. Mol Cell Biol 22(4):1094–1105
28. Zhu YH, Zhang CW, Lu L, Demidov ON, Sun L, Yang L, Bulavin DV, Xiao ZC (2009) Wip1 regulates the generation of new neural cells in the adult olfactory bulb through p53-dependent cell cycle control. Stem cells 27(6):1433–1442. doi:10.1002/stem.65
29. Sun S, Guo Z, Xiao X, Liu B, Liu X, Tang PH, Mao N (2003) Isolation of mouse marrow mesenchymal progenitors by a novel and reliable method. Stem cells 21(5):527–535. doi:10.1634/stemcells.21-5-527
30. Shreeram S, Demidov ON, Hee WK, Yamaguchi H, Onishi N, Kek C, Timofeev ON, Dudgeon C, Fornace AJ, Anderson CW, Minami Y, Appella E, Bulavin DV (2006) Wip1 phosphatase modulates ATM-dependent signaling pathways. Mol Cell 23(5):757–764. doi:10.1016/j.molcel.2006.07.010
31. Rosen ED, MacDougald OA (2006) Adipocyte differentiation from the inside out. Nat Rev Mol Cell Biol 7 (12):885–896. doi:10.1038/nrm2066
32. Barsh GS, Schwartz MW (2002) Genetic approaches to studying energy balance: perception and integration. Nat Rev Genet 3(8):589-600. doi:10.1038/nrg862
33. Armata HL, Chamberland S, Watts L, Ko HJ, Lee Y, Jung DY, Kim JK, Sluss HK (2015) Deficiency of the tumor promoter gene wip1 induces insulin resistance. Molecular endocrinology 29(1):28–39. doi:10.1210/me.2014-1136